Supporting Information for:

Interplay of Physically Different Properties Leading to Challenges in Separating Lanthanide Cations – an *Ab Initio* Molecular Dynamics and Experimental Study

Kevin Leung,* Anastasia G. Ilgen, and Louise J. Criscenti

Sandia National Laboratories, Albuquerque, NM 87185

Contents

I. HYDRATION NUMBERS AND HYDROLYSIS DYNAMICS

Fig. S1 depicts the pair correlation functions ($g_{\mathrm{Ln-O}}(r)$) between Lu(III) and Eu(III) and the oxygen sites of water molecules in a sampling window where the cations are far from the silica surface (Z_i=7.40 Å). Since these are not bulk-like aqueous simulation cells, we normalize $g_{\mathrm{Ln-O}}(r)$ using the mean first hydration shell coordination number against $4\pi \int dr r^2 g_{\mathrm{Ln-O}}(r)$ with the integration cut off r_c chosen to be 3.2 Å for both cations. This cut-off is also used to collect real-time coordination number statistics for Ln(III)-O bonds. The $g_{\mathrm{Ln-O}}(r)$ peak occurs at 2.30 Å and 2.40 Å for Lu(III) and the larger Eu(III) cation, respectively. They are similiar to values reported in the theoretical literature.[1–4] While the Lu(III) and Eu(III) $g(r)$ look similar, there is less probability that the Lu(III)-O distance is between 2.8-3.4 Å than for the Eu(III)-O distance.

Figures S2–S5 depict the time evolution of the mean hydration number N_{hyd} and the number of H_2O molecules hydrolysed into OH^- (N_{OH}) in the first hydration shell in different sampling windows. For O-H bonds, a distance criteria of 1.25 Å is adopted. In principle, N_{sio}, defined in the main text as the number of deprotonated SiO^- groups in the simulation cell, should equal the three minus N_{oh} on average. In practice, they may be slightly different because of H^+ in transit between the silica surface and the Ln(III) hydration shell.

The predicted Ln^{3+} hydrolysis behavior is consistent with acid-base studies in the literature. On the one hand, Yu *et al.*, using the DFT method and cluster models for hydrated Ln^{3+} complexes, have predicted pK_{a1} between 3 and 4 for Lu^{3+}. Since the SiOH groups in our model have pK_a=7 to 8.1, that cluster model work suggests that $Lu^{3+}(H_2O)_n$ is more acidic than SiOH and should donate a H^+ to one of the three SiO^- that initially exists before Lu^{3+} desorption. On the other hand, according to the Lawrence Berkeley PHREEQC thermodynamics database,[5] in the dilute Ln^{3+} limit at pH=6, $[Lu^{3+}OH^-]/[Lu^{3+}]\sim0.015$ while $[Eu^{3+}OH^-]/[Eu^{3+}]\sim0.0075$. Extrapolating the data available at lower pH to higher pH, we estimate that $pK_{a1}\sim8$, with Lu^{3+} being slightly more acidic. For Eu^{3+}, our AIMD simulations reveal no tendency towards hydrolysis far from the surface, which is more consistent with the PHREEQC database pK_{a1} values, and with Ref. 7, than those of Yu *et al.* To our knowledge, pK_{a1} of the hydrated Ln^{3+} complexes has not been computed using AIMD/PMF techniques similar to the way we computed pK_a on mineral surfaces.[8]

In some Lu^{3+} sampling windows with Z>5 Å, double deprotonation is observed during

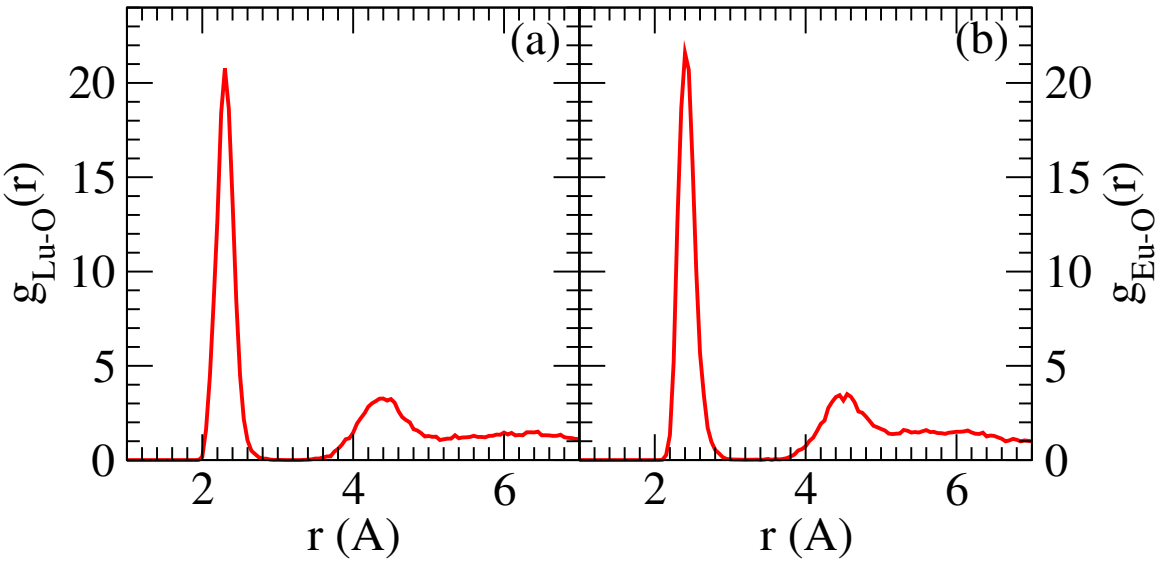

FIG. S1: Pair correlation function between Ln(III)-O_{water} sites in PMF sampling windows where Ln(III) ions are far from the silica slab. (a) Lu(III); (b) Eu(III).

a fraction of the trajectory (Fig. 3b of the main text). This does not appear consistent with the pK_{a2} values predicted in Ref. 6. However, the static $Ln^{3+}(H_2O)_7(OH^-)_2$ used in that calculation differ in stoichiometry from the $Ln^{3+}(H_2O)_5(OH^-)_2$ which spontaneously emerges in our solvation shell. It cannot be ruled out that the DFT technique we apply may also underestimate pK_{a2}.

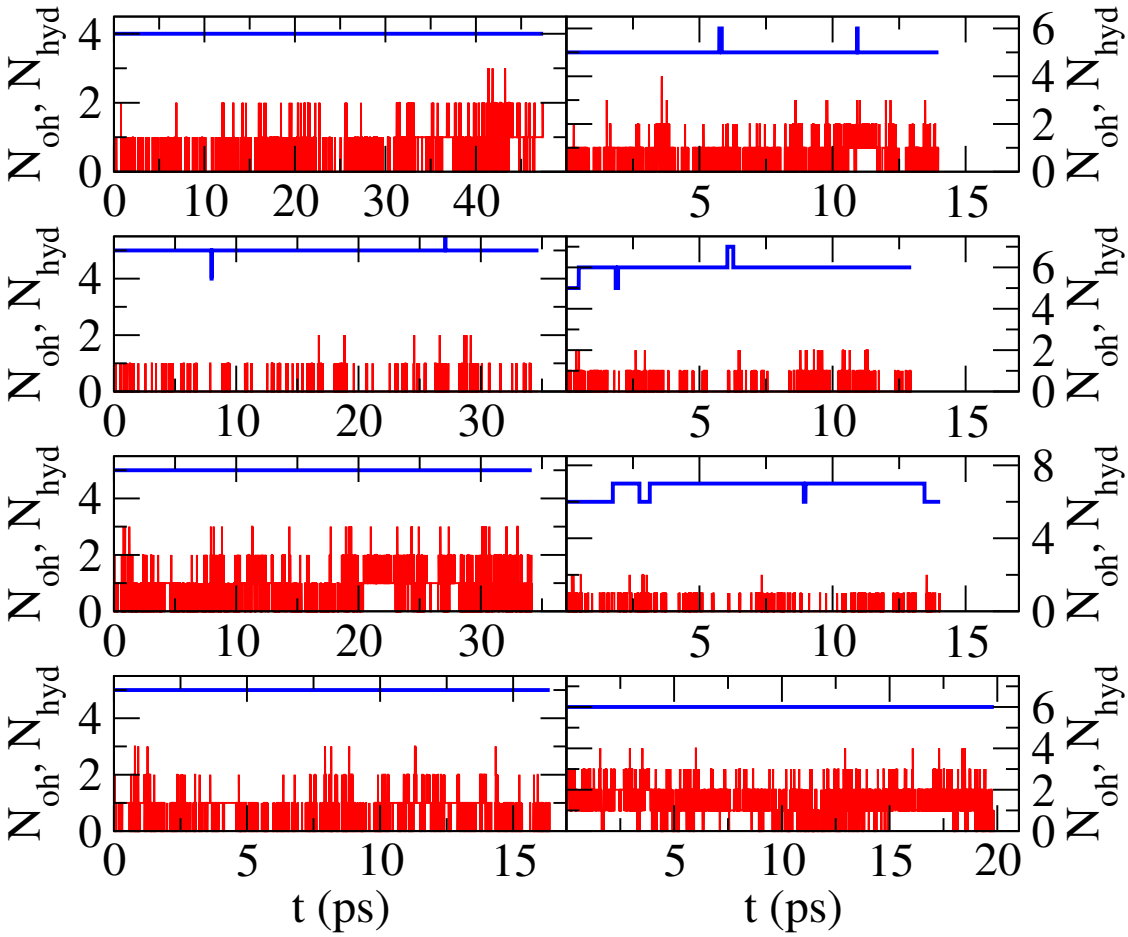

FIG. S2: Blue and red depict the real-time hydration number and number of hydrolysis events in each sampling window for Lu(III). From up to down on the left column and then right: unconstrained, Z_i=3.50 Å, 3.80 Å, 4.10 Å, 4.40 Å, 4.70 Å, 4.90 Å, and 5.30 Å, respectively.

II. MORE POTENTIAL-OF-MEAN-FORCE DETAILS

Trajectory lengths in different umbrella sampling window trajectories are given in Table S1.

In one Lu(III) window centered around Z_i=3.20 Å, only, the hydration number appears unconverged, and further calculations are conducted to the $\Delta W(Z)$ curve assembled across

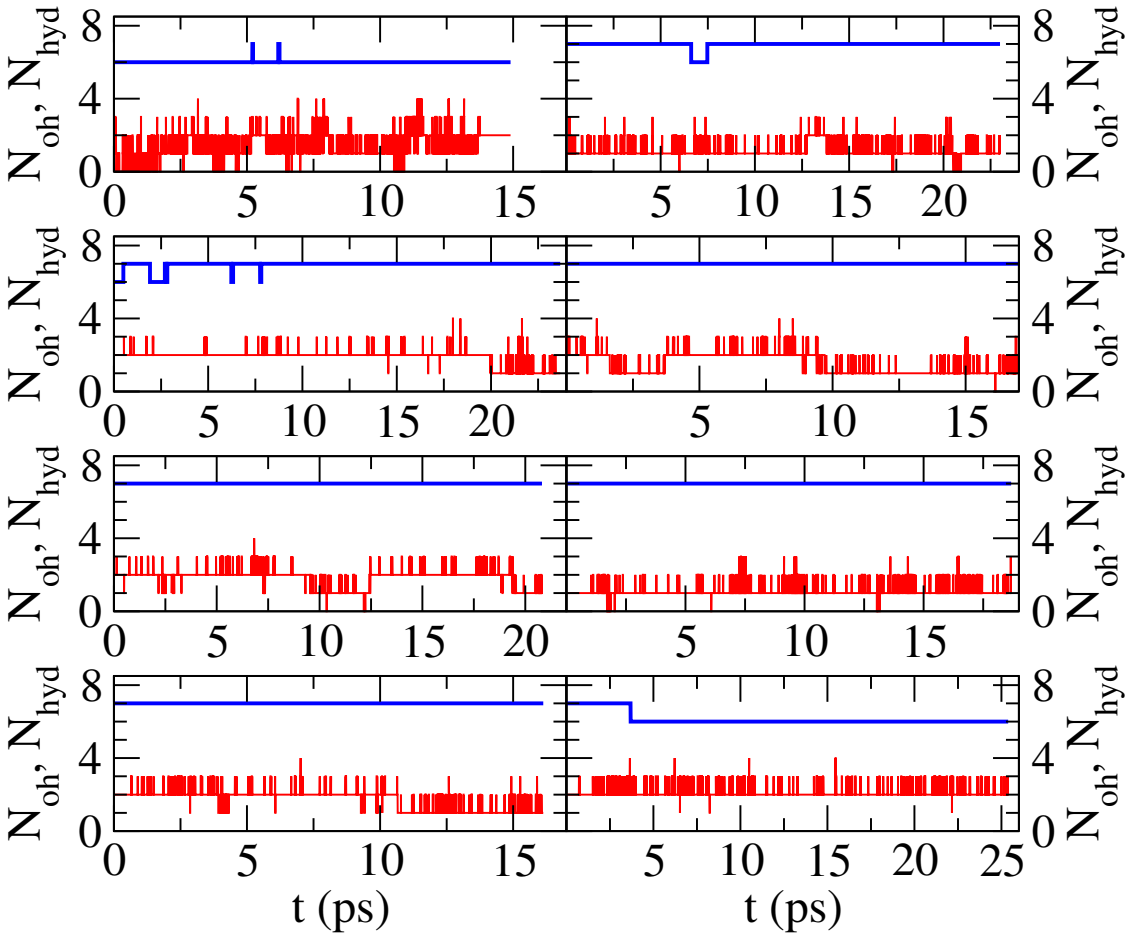

FIG. S3: Blue and red depict the real-time hydration number and number of hydrolysis events in each sampling window for Lu(III). Continued from Fig. S2. From up to down on the left column and then right: Z_i=5.60 Å, 5.90 Å, 6.20 Å, 6.50 Å, 6.80 Å, 7.10 Å, 7.40 Å, and 7.70 Å, respectively.

different Z_i windows in prelminary results has led us to re-examine N_{hyd} there. We initiate N_{hyd}=4 and 5 in parallel trajectories, which maintain these N_{hyd} values over their ∼15 ps durations. Then we perform a short, secondary PMF calculation by moving one H_2O from tne N_{hyd}=5 run to outside the solvation shell. Using this Lu(III)-O_{water} distance-based secondary reaction coordinate, we find that the N_{hyd}=5 trajectory is more favorable by 0.16 eV (Fig. S6). The Lu(III) $\Delta W(Z)$ curve shown in Fig. 2 of the main text reflect this

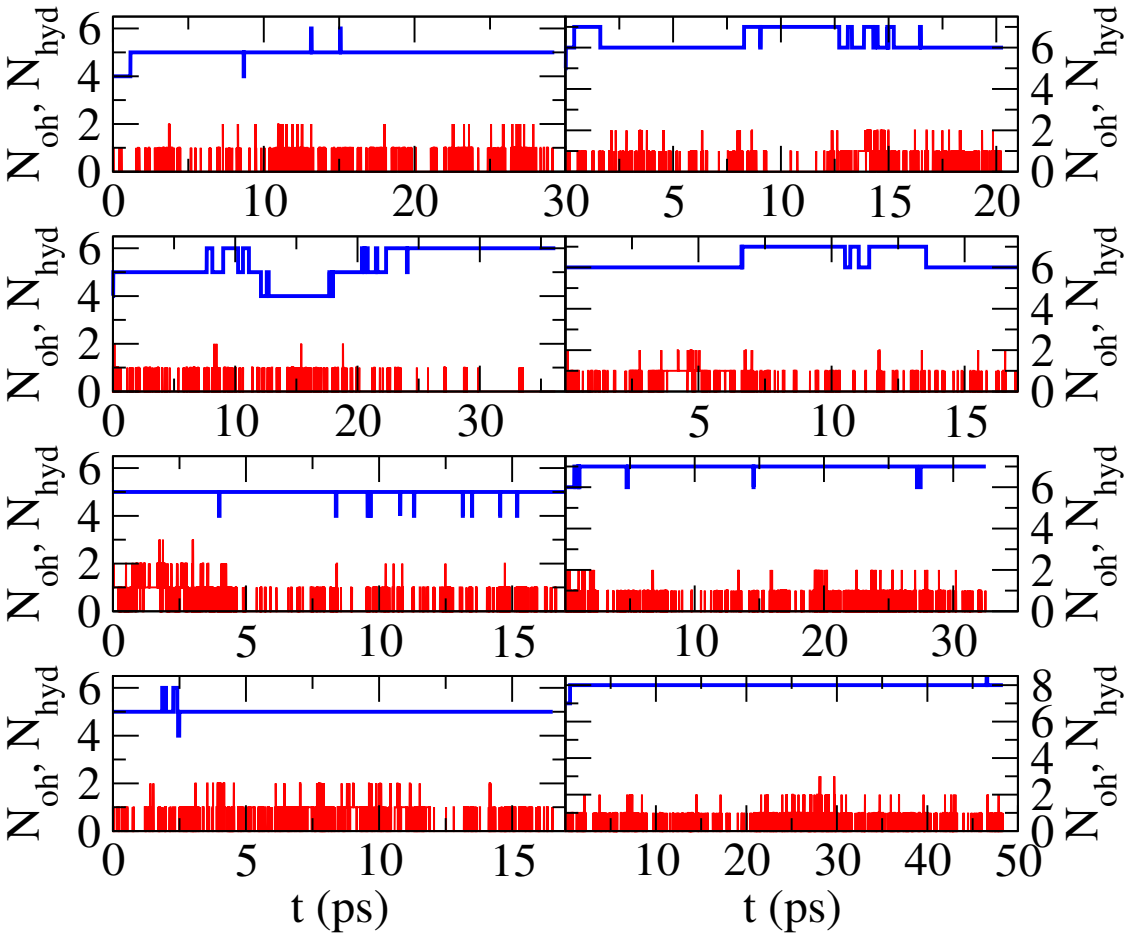

FIG. S4: Blue and red depict the real-time hydration number and number of hydrolysis events in each sampling window for Eu(III). From up to down on the left column and then right: unconstrained, Z_i=3.50 Å, 3.80 Å, 4.10 Å, 4.40 Å, 4.70 Å, 5.00 Å, and 5.30 Å, respectively.

choice in this one window. We stress that only this window seems problematic and requires special treatment.

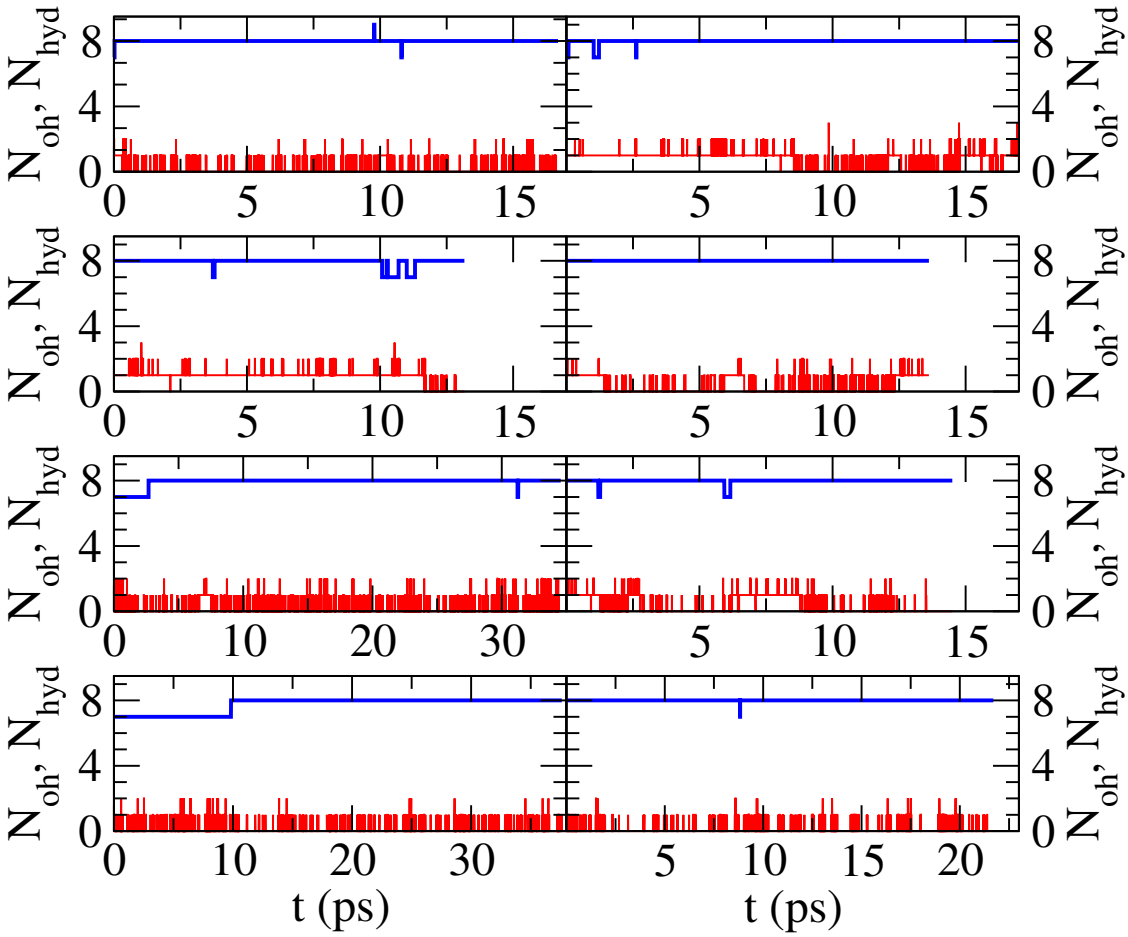

FIG. S5: Blue and red depict the real-time hydration number and number of hydrolysis events in each sampling window for Eu(III). Continued from Fig. S4. From up to down on the left column and then right: Z_i=5.60 Å, 5.90 Å, 6.20 Å, 6.50 Å, 6.80 Å, 7.10 Å, 7.40 Å, and 7.70 Å, respectively.

III. DFT+U JUSTIFICATION FOR USING THE EU(A) PSEUDOPOTENTIAL

This section revisits Sec. IIID of the main text. The systems depicted in Fig. 5a-b of the main text represent convenient platforms to examine the validity of the Eu(A) pseudopotential used, which omits f-electrons. Here we apply DFT+U[9] at various (U-J) values to compute the Eu(B)-predicted binding energies of a Eu^{3+} to the $Si_{40}O_{88}H_{13}^{3-}$ slab relative

cation	Z_i	$t_{\rm tot}$	Z_i	$t_{\rm tot}$	Z_i	$t_{\rm tot}$
Lu(III)	uncon.	47.4	3.20	16.0	3.50	34.7
	3.80	17.8	4.10	16.4	4.40	14.0
	4.70	12.8	4.90	14.0	5.30	19.8
	5.60	14.9	5.90	23.7	6.20	20.8
	6.50	16.1	6.80	23.0	7.10	17.0
	7.40	18.7	7.70	25.4	8.00	12.8
Eu(III)	uncon.	40.5	3.20	19.2	3.50	36.2
	3.80	20.0	4.10	16.5	4.40	20.3
	4.70	18.0	5.00	32.5	5.30	48.3
	5.60	16.7	5.90	13.2	6.20	34.5
	6.50	37.6	6.80	17.0	7.10	16.5
	7.40	14.5	7.70	29.3		

TABLE S1: Details of umbrella sampling AIMD trajectories with constraining potentials $A_o(Z - Z_i)^2$. Z_i is in Å. $t_{\rm tot}$ is the trajectory length used in sampling statistics, in picoseconds. The harmonic prefactor A_o=2 eV. Secondary umbrella sample is applied to Lu(III) and Eu(III) at Z_i=4.9 Å and 5.0 Å, respectively (see text).

to Lu^{3+}, using the Eu(A) value as a reference. This difference is designated $\Delta\Delta E$. As mentioned in the main text, if both Eu pseudopotentials are equally accurate, the energy difference ($\Delta\Delta E$) between them should be zero. Instead, we find that the Eu(B) result is favored by $\Delta\Delta E$=-0.73 eV.

In the main text, we argue that switching to DFT+U should improve the agreement between Eu(A) and Eu(B). Setting U-J=4.5 eV. We find that ΔE=-0.13 eV, -0.11 eV, and -0.04 eV with 1-3 H_2O in the simulation cell. Therefore the Eu(A) pseudopotential yields predictions very similar to Eu(B), with f-electrons – as long as the more reliable[10] DFT+U augmentation is applied to f-electrons in the latter case. (Eu(A) does not have f electrons and DFT+U is inapplicable there.) Note that the Eu(A) and Eu(B) pseudopotentials have also been shown to yield similar structural properties when the latter is used in conjunction with DFT+U augmentation.[11]

However, here we show that DFT+U results slightly vary with the value of (U-J). Ta-

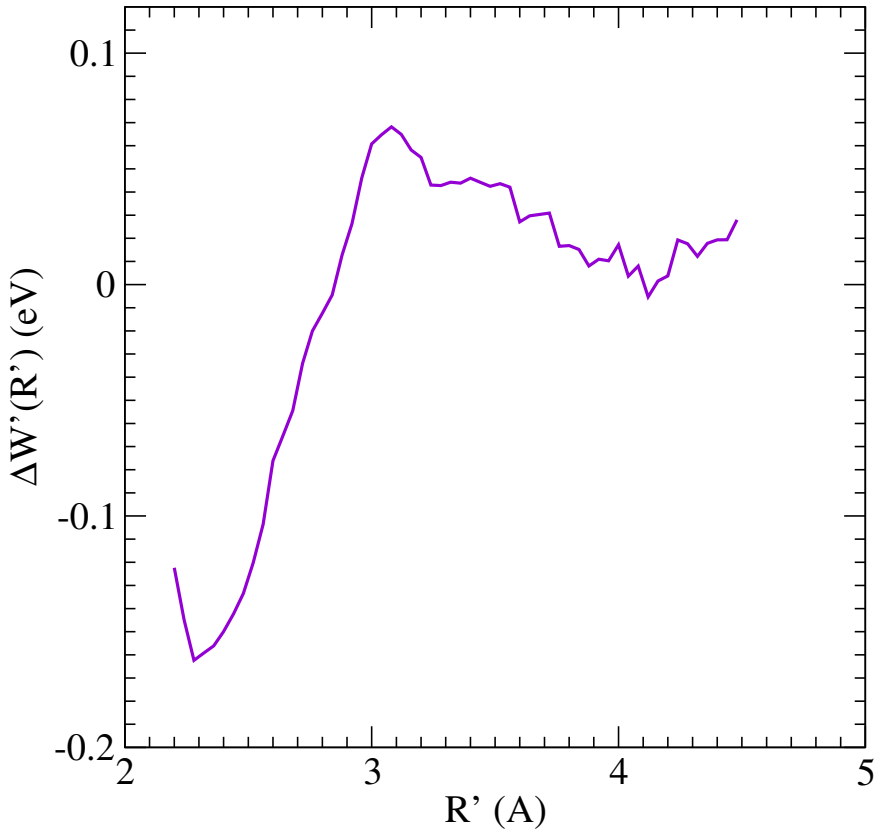

FIG. S6: $\Delta W'(R')$ for moving a H_2O molecule from the Lu(III) PMF window with R_i=3.5 Å, with 5 and 4 H_2O in the Lu(III) hydration shells at small and large R', respectively. While the statistics can be improved, and this calculation does not strictly speaking treat all H_2O molecules as identical, it is clear that 5-coordination is more favorable.

ble S2 shows that, for the configuration associated with Fig. 5a-b of the main text, $\Delta\Delta E$ ranges from -0.13 eV to +0.05s eV as (U-J) varies from 4.5 eV to 6.5 eV. The variation is not large but is significant compared to the desorption free enegy difference between Lu^{3+} and Eu^{3+}, which is 0.03 eV. Hence, in the main text, we switch to the HSE06 hybrid functional. HSE06 results are included in Table S2 for completeness. Note that the Eu(A) and Eu(B) HSE06 $\Delta\Delta E$ differ by 0.16 eV. We speculate that this could be because the Eu(A) pseudopotential, with no $4f$ electrons, was more restricted in its range of application and was more suited to be used with the PBE functional.

method	PBE*	PBE	HSE06*	HSE06
$\Delta\Delta$ E	0.00	-0.70	-0.23	-0.07
method	(U-J)=2.5	(U-J)=4.5	(U-J)=5.5	(U-J)=6.5
$\Delta\Delta$ E	-0.48	-0.13	-0.06	+0.05

TABLE S2: Difference in Ln^{3+}silica binding energies between Lu^{3+} and Eu^{3+}, with one H_2O molecule, referenced to the Eu(A) PBE value, for the configuration depicted in Fig. 5a-b of the main text. All energies are in units of eV. Eu(B) is used in all calculations except those marked with an $*$.

[1] M. Hitzenberger, T.S. Hofer and A.K.H. Weiss, *J. Chem. Phys.* 2013, **139**, 114306.

[2] V. Migliorati, A. Serva, F.M. Terenzio and P. D'Angelo, *Inorg. Chem.* 2017, **56**, 6214-6224.

[3] M. Hitzenberger, T.S. Hofer and A.K.H. Weiss, *J. Chem. Phys.* 2013, **139**, 114306.

[4] L.R. Canaval and B.M. Rode, *Chem. Phys. Lett.* 2015, **618**, 78-82.

[5] LLNL PHREEQC database. Johnson, J.; Anderson, F.; Parkhurst, D.L. Database thermo.com.V8.R6.230, Rev 1.11. Lawrence Livermore National Laboratory, Livermore, California; 2000.

[6] D. Yu, R. Du, J.-C. Xiao, S. Xu, C. Rong and S. Liu, *J. Phys. Chem. A* 2018, **122**, 700-707.

[7] D. Garcia, J. Lützenkirchen, V. Petrov, M. Siebentritt, D. Schild, G. Lefevre, T. Rabung, M. Altmaier, S. Kalmykov, L. Duro and H. Geckeis, *Coll. Surfaces A* 2019, **578**, 123610.

[8] K. Leung and L.J. Criscenti, *J. Phys. Condens. Matter* 2012, **24**, 124015.

[9] S.L. Dudarev, G.A. Botton, S.Y. Savrasov, C.J. Humphreys and A.P. Sutton. *Phys. Rev. B*, 1998, **57**, 1505.

[10] S. Lutfalla, V. Shapovadov and A.T. Bell, *J. Chem. Theoy Comput.* 2011, **7**, 2218-2223.

[11] D.J. Vogel, D.F. Sava Gallis, T.M. Nenoff and J.M. Rimsza, *Phys. Chem. Chem. Phys.* 2019, **21**, 23085.